Received: 28 February 2024 | Revised: 4 July 2024 | Accepted: 8 July 2024

DOI: 10.1002/asl.1260

RESEARCH ARTICLE

Atmospheric Science Letters RMetS

Changing dynamics of Western European summertime cut-off lows: A case study of the July 2021 flood event

Vikki Thompson[1] | **Dim Coumou**[1,2] | **Vera Melinda Galfi**[2] | **Tamara Happé**[2] | **Sarah Kew**[1] | **Izidine Pinto**[1] | **Sjoukje Philip**[1] | **Hylke de Vries**[1] | **Karin van der Wiel**[1]

[1]Royal Netherlands Meteorological Institute (KNMI), De Bilt, The Netherlands

[2]Institute for Environmental Studies, Vrije Universiteit Amsterdam, Amsterdam, The Netherlands

Correspondence
Vikki Thompson, Royal Netherlands Meteorological Institute (KNMI), De Bilt, The Netherlands.
Email: vikki.thompson@knmi.nl

Funding information
Horizon 2020 Framework Programme (XAIDA Project), Grant/Award Number: 101003469; Koninklijk Nederlands Meteorologisch Instituut (MSO-ExtremeWeather)

Abstract

In July 2021, a cut-off low-pressure system brought extreme precipitation to Western Europe. Record daily rainfall totals led to flooding that caused loss of life and substantial damage to infrastructure. Climate change can amplify rainfall extremes via thermodynamic processes, but the role of dynamical changes is uncertain. We assess how the dynamics involved in this particular event are changing using flow analogues. Using past and present periods in reanalyses and large ensemble climate model data of the present-day climate and 2°C warmer climate, we find that the best flow analogues become more similar to the cut-off low-pressure system observed over Western Europe in 2021. This may imply that extreme rain events will occur more frequently in the future. Moreover, the magnitude of the analogue lows has deepened, and the associated air masses contain more precipitable water. Simulations of future climate show similar events of the future could lead to intense rainfall further east than in the current climate, due to a shift of the pattern. Such unprecedented events can have large consequences for society, we need to mitigate and adapt to reduce future impacts.

KEYWORDS

atmospheric and climate dynamics, change and impacts, climate variability, weather/climate extremes

1 | INTRODUCTION

In July 2021, a persistent low-pressure system caused extreme precipitation in parts of Germany, Belgium, the Netherlands and Luxembourg (Mohr et al., 2023; Tradowsky et al., 2023; Figure 1). The flooding caused at least 220 deaths, mostly in Germany (Koks et al., 2022). Infrastructure damage included hospitals, roads, bridges and utility networks, with an estimated total damage of EUR 46 billion (Mohr et al., 2023). Precipitation was greatest on 14 July, with daily rainfall totals of 150 mm in parts of Western Germany (Mohr et al., 2023; Figure 1). In this study, we investigate the changing dynamics of such events in past, present and future climates.

Extreme summer rainfall in Western Europe is becoming more frequent and intense (Seneviratne et al., 2021;

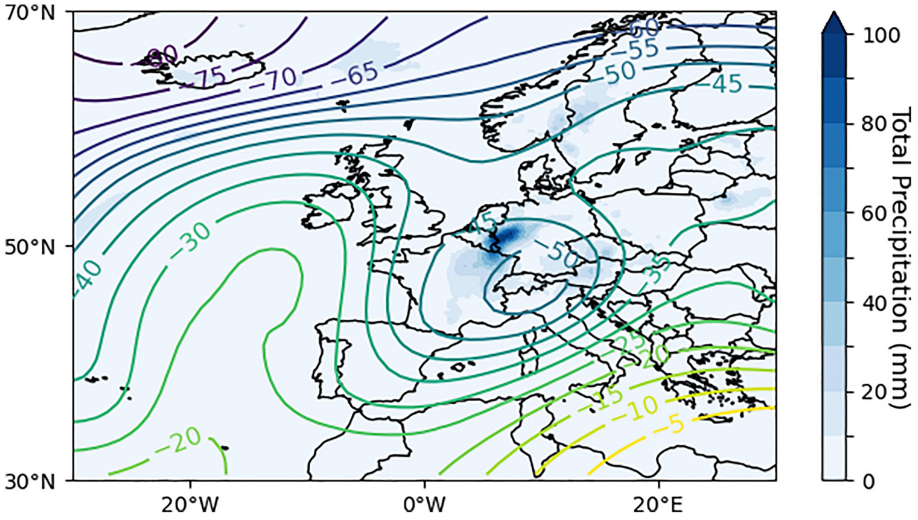

FIGURE 1 The observed meteorological situation of 14 July 2021. Daily precipitation and 250 hPa streamfunction over Western Europe on 14 July 2021, the day of peak rainfall from the event, from ERA-5 reanalysis data. Contour lines show the 250 hPa streamfunction ($\times 10^6$ m^2/s), shading shows the daily precipitation totals (mm).

van de Vyver et al., 2023). Climate change driven intensification of the water cycle increases daily rainfall extremes (Fischer & Knutti, 2016; Fowler et al., 2021). In some regions, the rate of increase is more than the Clausius–Clapeyron rate of 7% per 1°C of warming (Fowler et al., 2021; van der Wiel et al., 2017; van Oldenborgh et al., 2017). The observed increase in extreme summer precipitation increases flood risks, illustrated by the many severe floods in Europe in summer 2023, including the Emilia-Romagna region of Italy in May, Romania and Serbia in June and Norway and Sweden in August (Europe—FloodList; Copernicus). Climate projections indicate that this trend will continue as global mean surface temperature increases (Kahraman et al., 2021; Masson-Delmotte et al., 2021; Rajczak & Schär, 2017).

Many climate extremes can be firmly attributed to human causes through thermodynamical changes alone (Seneviratne et al., 2021; van Oldenborgh et al., 2022). For heavy rainfall this is difficult due to the complexity of rainfall simulations and model uncertainties (Tradowsky et al., 2023). Despite the challenges, studies have shown anthropogenic emissions have increased the likelihood of many extreme rainfall events, such as those associated with flooding in France in May 2016 (Philip et al., 2018) and in the United Kingdom in December 2015 (Otto et al., 2018). Although a warmer climate will, on average, intensify extreme precipitation events, the location and frequency depends on atmospheric circulation changes (Seneviratne et al., 2021). Statistically fitting generalised extreme value distributions to climate data assess the effects of both dynamical and thermodynamical changes, with no separation of drivers. The methods used assume a dependency on global mean temperature, but for some extreme events, such as those including convective rainfall (Fowler et al., 2021), dynamical feedbacks or changes in large-scale circulation lead to non-linear scaling with global mean temperature—and large uncertainties in attribution statements. Tradowsky et al. (2023) found the July 2021 event 1.2–9 times more likely than in preindustrial, a range of almost an order of magnitude. As extreme weather events increase at a rate which exceeds thermodynamical expectations, it becomes ever more important to understand the role of dynamics (Di Capua & Rahmstorf, 2023).

We focus on the July 2021 extreme rainfall, which was associated with a cut-off low-pressure system (Figure 1). This created large-scale atmospheric flow conditions, which caused extreme, persistent rainfall. Analogues of large-scale dynamics allow conditional attribution of the intensity of the extreme and assessment of changes in likelihood (Yiou et al., 2013). Faranda et al. (2022) investigated the July 2021 event using a reanalysis of sea level pressure data, finding little change in the intensity of the low-pressure system, only a moderate increase in temperature and an increase in precipitation consistent with increasing water vapour in a warmer atmosphere.

In this study, we investigate how the atmospheric circulation patterns associated with the July 2021 event are changing as the world warms. Assessing both reanalysis data and a large ensemble of climate model simulations we can go beyond Faranda et al. (2022), investigating both past changes and projected future changes. We assess changes in the characteristics of events, evaluating the frequency, intensity and persistence of the analogues. Understanding how the dynamics of such events is changing will allow better preparation to reduce impacts of future events.

2 | METHODS

2.1 | Data

We use the fifth-generation ECMWF atmospheric reanalysis of the global climate (ERA-5) dataset as a proxy for

TABLE 1 Climate data periods used in this study.

Dataset	Period 1	Period 2
ERA-5	Past: 1950–1979	Present: 1993–2022
KNMI–LENTIS	Present: 2000–2009	Future: 2075–2084 in SSP2-4.5

observations (Bell et al., 2021). To assess possible future changes in these rare event types, we use the large ensemble climate modelling dataset KNMI–LENTIS (KNMI Large ENsemble TIme Slice) generated with EC-Earth3_p5 (Muntjewerf et al., 2023a). This fully coupled global climate model with atmosphere, ocean, sea ice and land components has ~80 km resolution (Döscher et al., 2022). The CMIP6 version of EC-Earth3 has a warm bias in the Southern Hemisphere and a cold bias in the Northern Hemisphere. It was retuned for the Dutch National Climate Scenarios (van der Wiel et al., 2024), leading to a smaller bias in the North Atlantic/European sector. KNMI–LENTIS covers two time periods: the present-day (2000–2009) and a +2K future (2075–2084 in Shared Socioeconomic Pathway 2-4.5 (SSP2-4.5)). Each 10-year period has 160 ensemble members, providing 1600 years of data. It is assumed that the 10-year periods do not show significant forced climate change, and ensemble size samples the full climate variability distribution.

For both ERA-5 and KNMI–LENTIS the climate variables used in this study are daily precipitation, and 250 hPa u- and v-wind components. Summertime (June–July–August) data are used from ERA-5 periods: 1950–1979 (past) and 1993–2022 (present), and the KNMI–LENTIS periods: 2000–2009 (present) and 2075–2084 (future) (Table 1). The model is regridded to the ERA-5 grid, with 1° resolution for the wind and 1/4° for precipitation.

We use the 250 hPa streamfunction to identify analogues, this is preferable over the use of geopotential height, as tropospheric warming will have led to an increase in geopotential height, which would require additional steps such as detrending (Faranda et al., 2022; Noyelle et al., 2023). The streamfunction field is calculated using Climate Data Operators using the equations:

$$u_r = +\frac{1}{r^2 \sin\theta}\frac{\partial \psi}{\partial \theta} \text{ and } u_\theta = -\frac{1}{r \sin\theta}\frac{\partial \psi}{\partial \rho},$$

where u_r and u_θ are the daily 250 hPa zonal and meridional velocity components, r is radial distance from the origin and θ the zenith angle in spherical coordinates (Schulzweida, 2023).

2.2 | Identifying analogues

Here, an analogue is defined as a day with similar upper-level atmospheric circulation to 14 July 2021 (Jézéquel et al., 2018). This event date was the peak rainfall day of the event (Figure 1). We use the region 30° N–70° N, 30° W–30° E to define analogues to represent the large-scale dynamics of the event. A smaller domain, more focussed on the cut-off low, may lead to more cut-off lows being included in the analogues, but could also lead to a failure to identify relevant changes to the larger scale circulation. We tested the impact of a smaller domain, finding no change in the sign of the trends or general pattern identified over the impacted region.

For the region, we calculate the pointwise Euclidian distance of the 250 hPa streamfunction field between the event date and each individual summer day by the equation:

$$\mathrm{ED} = \sqrt{\left(A_{x_1,y_1} - B_{x_1,y_1}\right)^2 + \left(A_{x_1,y_2} - B_{x_1,y_2}\right)^2 + \ldots + \left(A_{x_n,y_n} - B_{x_n,y_n}\right)^2},$$

where ED is Euclidean distance between 2D-fields, A_{xy} (event date) and B_{xy} (any other date). We use Euclidean distance over alternatives such as spatial rank correlation, as it favours larger structures and assesses the overall proximity of maps in terms of mean state, not only spatial pattern (Yiou et al., 2013). For each of the periods, we take the 30 days with the smallest Euclidean distances compared to the event as our analogue set. We impose a gap of 5 days between the analogues, resulting in 30 unique events. For the present-day ERA-5 period, the event itself is excluded from analogues.

We perform significance testing on the composites. For each gridpoint, two-sided t-tests (assuming equal variance) are used, if the $p < 0.05$ the distributions are assumed to differ significantly (Figure 2d,g). Note, we take 30 analogues from each period, despite KNMI–LENTIS containing many more days to select from than ERA-5. We take advantage of the large ensemble to assess more similar events than is possible with ERA-5 alone. We tested the impacts of the choice to use only 30 analogues from the model, rather than the same proportion (Figure S1). We find the same proportion does not give composites equally similar to the event—differences are larger in the model. This suggests the dynamical situation of the event is less likely in the model than in observations.

2.3 | Calculating analogue typicality and persistence

To assess analogue similarity between periods we calculate analogue typicality (T). This metric is similar to the

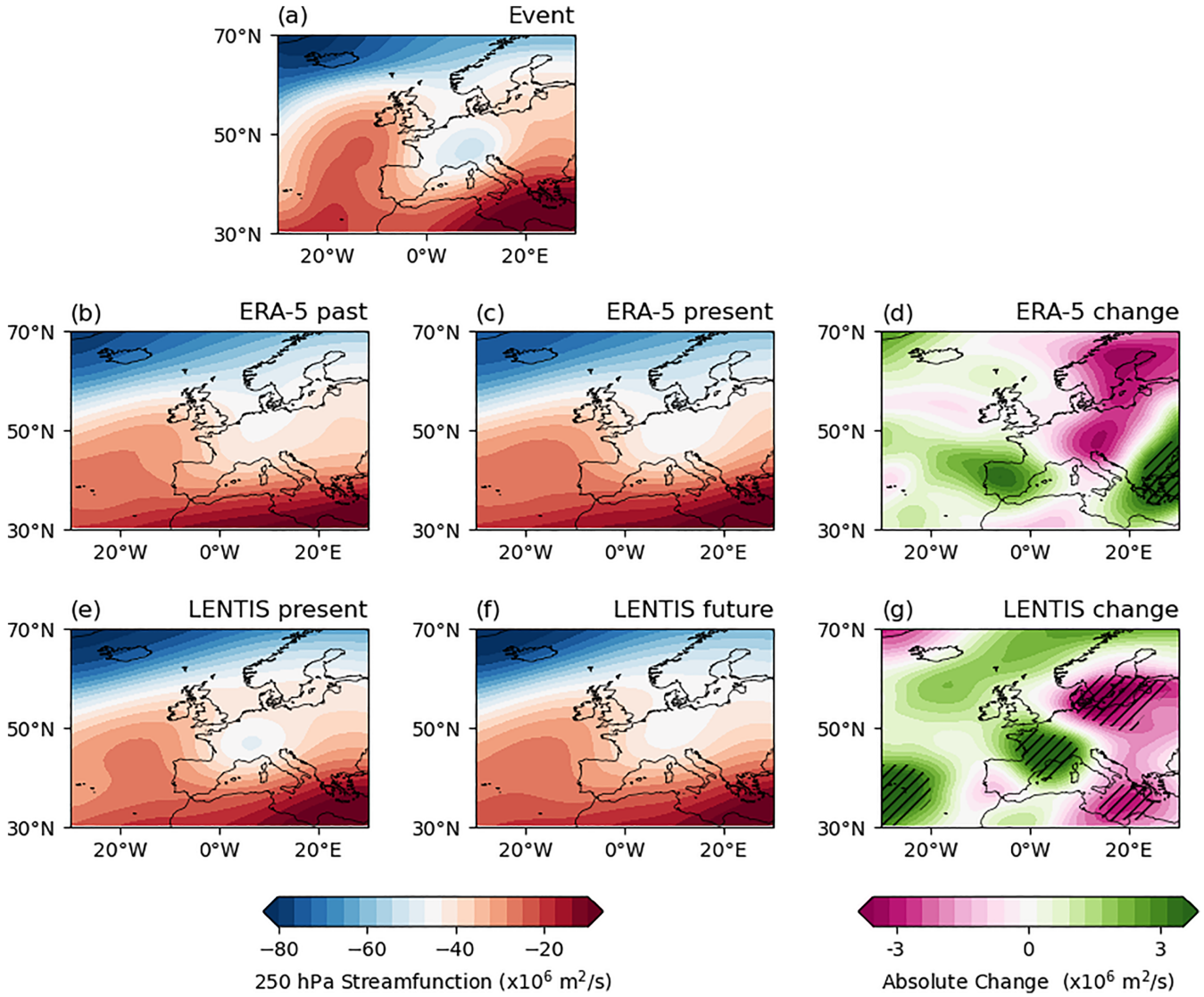

FIGURE 2 Composites of the analogue set for 14 July 2021. (a) The atmospheric circulation (250 hPa streamfunction, $\times 10^6$ m^2/s) of the observed event, 14 July 2021. (b, c) The composites of the closest 30 analogue days from ERA-5, past (1950–1979) and present (1993–2022). (d) The difference between the past and present. Hashed regions indicate a statistically significant difference between the time periods, calculated using a pointwise 2-sided Welch's *t*-test with $p < 0.05$ significant. (e–g) As in (b–d), but for the LENTIS data, present (2000–2009) and future (2075–2084 in SSP2-4.5; 2K warmer).

analogue quality used by Faranda et al. (2022). T_{event} is calculated for each analogue set as the inverse of the sum of the 30 Euclidean distances. $T_{analogue}$ is also calculated for each of the analogues, by identifying their 30 closest analogues within the same period and calculating the inverse sum of the Euclidean distances of those. Thus, we get a value of T_{event} and a $T_{analogue}$ distribution (30 values) for each period (Figure 3a,b). Higher T_{event} indicates that analogues are more similar to the event. Comparing T_{event} for different periods allows an assessment of whether the atmospheric circulation enters the phase space of the event more or less frequently in each period—a higher T_{event} indicates the pattern is more typical and lower more unusual.

Statistical significance of the difference between T_{event} in periods is calculated by two-sided Welch's *t*-tests on the two distributions of Euclidean distances for analogues of each period, $p < 0.05$ is significant for the distributions of $T_{analogue}$ significance is calculated the same way on the distributions themselves.

If T_{event} is within the $T_{analogue}$ distribution the event is deemed to have good analogues, but if T_{event} is smaller than the $T_{analogue}$ distribution then the atmospheric circulation pattern of the event is highly unusual—the analogues themselves are more similar to each other than to the event. In this case the event is an outlier, analogues will not be useful for assessing dynamical changes.

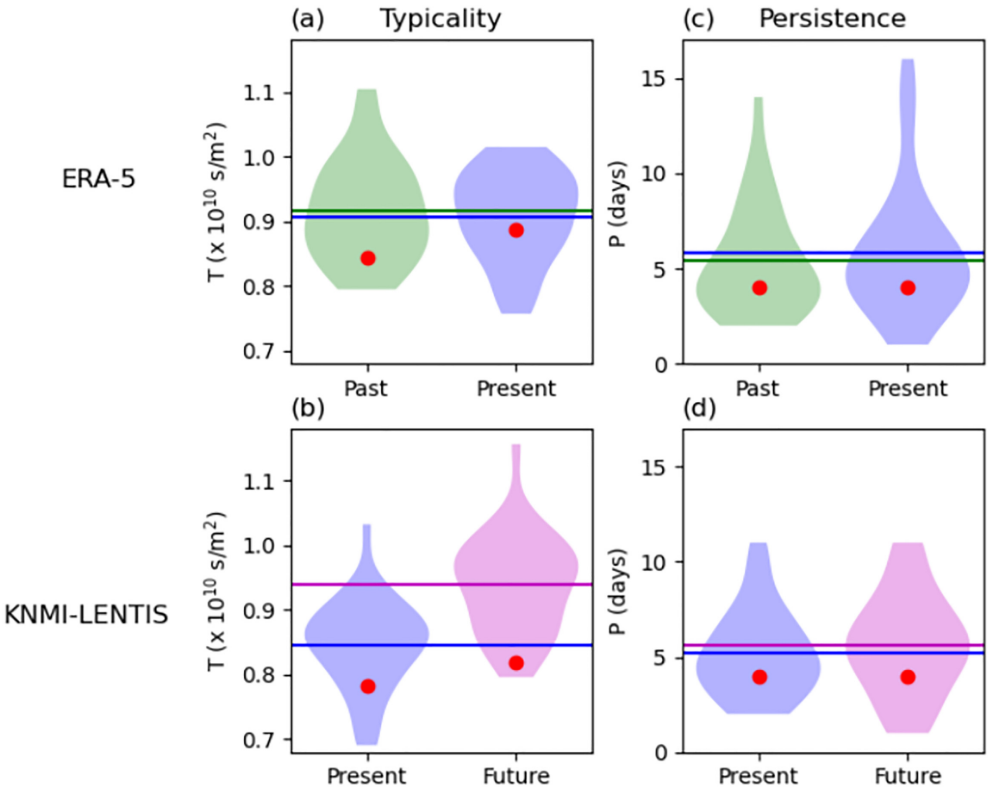

FIGURE 3 Analogue typicality and persistence (a) showing the distribution of $T_{analogue}$ (violin plots) and the T_{event} (red point) for the ERA-5 past (1950–1979) and present (1993–2022) periods. Horizontal lines indicate the means of the $T_{analogue}$ distributions (b) as in (a) for the present and future KNMI–LENTIS periods. (c) showing the distribution of $P_{analogue}$ (violin plots) for ERA-5 past and present and P_{event} (red points), and $P_{analogue}$ distributions means (d) as in (c) for the present and future KNMI–LENTIS periods.

We assess whether persistence of such events over Western Europe is changing. Persistence is assessed by calculating spatial correlation between the event and neighbouring days over the same domain and field as analogues; the event persists if the spatial correlation coefficient is >0.9, the number of continuous days meeting this criterion (both preceding and succeeding the event) is the event persistence, P_{event}. This is calculated for each individual analogue from the analogue sets to give distributions: $P_{analogue}$.

3 | RESULTS

All four analogue sets, ERA-5 past and present periods and KNMI–LENTIS model present and future periods, show a low-pressure over the region matching the observed event (Figure 2a–c), though not all analogues show a distinct cut-off low (Figures S4–S12). We find ~50% of the reanalysis analogues exhibit cut-off lows, whereas ~70% of the model analogues do. As the model dataset is larger it is unsurprising that the composites are more similar to the event, but investigating the same proportion of events it appears the model has a smaller proportion of similar days (Figure S1). There are differences between the reanalysis and model analogues—as would be expected due to model biases and the different sizes of the periods (Muntjewerf et al., 2023a). The model biases appear to cause an underestimation in the frequency of event-like flows identified as analogues.

The differences between the composites of past and present analogues from reanalysis shows how the intensity of events similar to July 2021 has changed (Figure 2d). For the model, where we compare present to future projections, we also detect a deepening trend. In contrast to ERA-5, this projected future trend is statistically robust. The consistency in the trend in both datasets provides evidence that it may be a long-term trend. There is an increased gradient across Europe from southwest to northeast. In central Europe, the area of greatest change shows $>3 \times 10^6$ m^2/s deepening (pink region in Figure 2d,g). In the model there is a statistically significant eastward shift in the low-pressure region, deepening further northeast, across Northern Germany (Figure 2e–g). Changes in the low-pressure system show similarities in both reanalysis and model, with $>3 \times 10^6$ m^2/s decrease in central Europe.

We can assess if the composites are becoming more similar to event over time (Figure S2). The low pressure is deeper in the event than in the composites for all periods. Thus, any deepening over time (Figure 2) increases the similarity with the event. This is also shown by the $T_{analogue}$ distributions (Figure 3), which show the analogues are becoming more like the event. Note, as analogues are chosen based on similarity to the event, we may not be identifying the most extreme low-pressure systems—just the most similar.

We assess how T_{event} changes within each period (Figure 3a,b). From past to present (reanalysis) and from present to future (model) we see that T_{event} (indicated by a red point) increases—the analogues are becoming statistically more similar to the event with time. We are investigating an extreme event, and for some such events there may be no other events that are similar. In such cases, there would be little value in investigating the flow analogues. We can use the distribution of $T_{analogue}$ to ensure that the event is not an outlier. In this study, we find that T_{event} lies within the $T_{analogue}$ distribution, thus concluding that the analogues are useable for assessing dynamical changes.

We find that the streamfunction of the event becomes more typical through time (T_{event} increases), and the analogues themselves are also more typical in later periods ($T_{analogue}$ increases). The latter is particularly true for the model (Figure 3b), where the difference between present and future typicality is statistically significant (two-sided Welch's t-test $p = 1.19 \times 10^{-5}$). This suggests that the frequency of such events has increased, enabling more similar events to be identified. There is an apparent model bias leading to an underestimation in the frequency of flow analogues, with less similar events identified in the model when the same proportion of analogues are used for both model and reanalysis (Figure S1). This is also evident in Figure 3a,b, where the typicality of both reanalysis and model are similar absolute values despite differing proportions of analogues.

To assess changes in event length, we use the persistence measure, P. P_{event} is 4 days (Figure S3). We compare this to the persistence of the analogues, $P_{analogue}$ (Figure 3c,d). We find that P_{event} lies within the distribution of $P_{analogue}$, but some analogues show much higher persistence, up to 16 days. Analogue events with much longer persistence do not show distinct cut-off lows and so are not associated with intense rainfall (Figure S3). Even events with a persistent cut-off low will not necessarily lead to rainfall increase as many other factors, such as moisture source, will affect this. There is no significant difference between different periods, suggesting no change in persistence through time. The model does not show analogues with as long persistence as the reanalysis. This appears to be because the model analogues are more similar to the event itself as there are more model days to sample from. This was tested by identifying the same proportion of analogues for the model and randomly sampling a distribution of 30 model events, these give a persistence distribution in closer agreement to ERA-5 results, with some even longer persistence events (Figure S4).

Analogue sets are identified from the regional dynamics alone, but we can assess the hemispheric patterns associated with the event (Figure 4a–e). Consistent

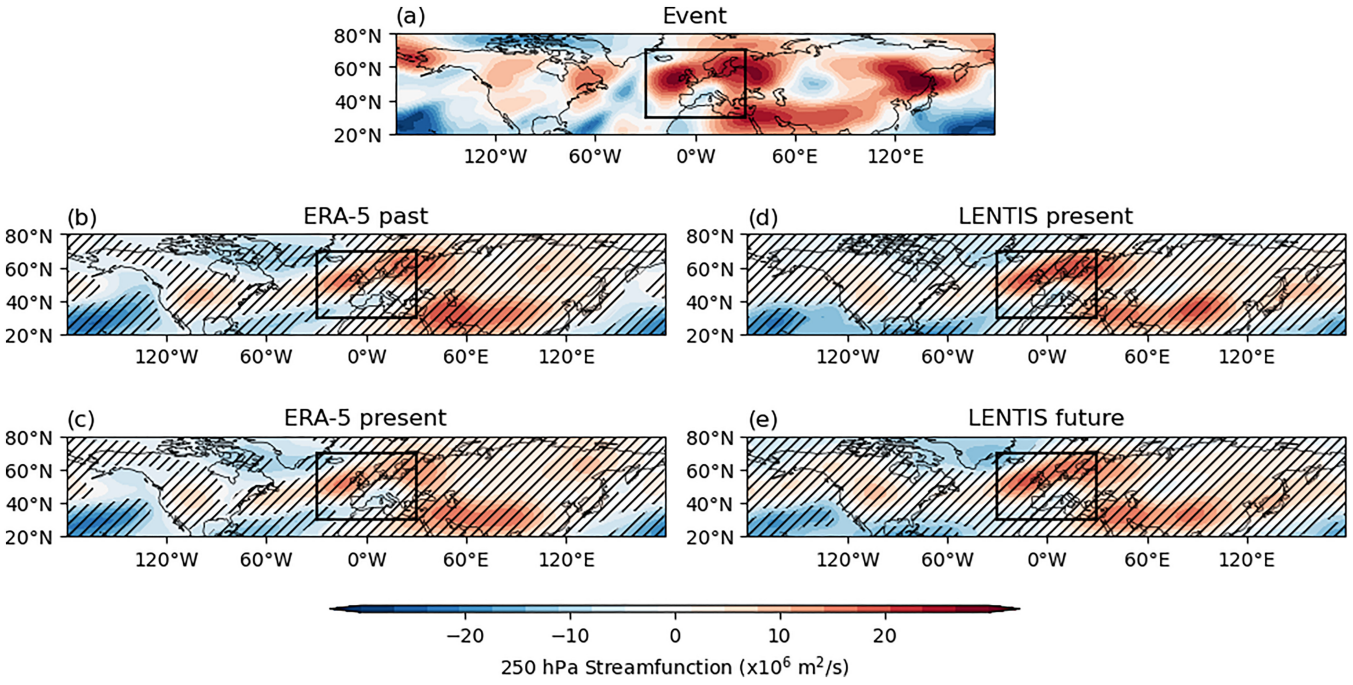

FIGURE 4 Large-scale dynamics of analogue events. (a) The 250 hPa streamfunction anomaly, with zonal mean relative to 1950–2023 removed, in $\times 10^6$ m^2/s, of the observed event, 14 July 2021. (b) The composite of the 250 hPa streamfunction anomaly with zonal mean removed, relative to 1950–1979, in $\times 10^6$ m^2/s, for the closest 30 analogue days from ERA-5, past (1950–1979). Hashed regions show where the signal in the composite of analogues is statistically different to zero, using a one-sided t-test ($p < 0.05$). (c) As in (b) for ERA-5 present day (1993–2022). (d, e) As in (b, c), but for the KNMI–LENTIS data, present (2000–2009) and future (2075–2084 in SSP2-4.5; 2K warmer).

patterns on this larger scale, either within analogue sets or with the event, indicate that global wave patterns may play a role. For the event, it appears that the dynamic situation over Europe was part of hemispheric atmospheric wave activity (Figure 4a). There are similarities between the event and the analogues, all show consistent high-pressure anomalies over North America and the North Pacific, though no analogue sets capture the high–low–high pattern shown in the event over the North Atlantic. ERA-5 analogues from both time periods show consistent patterns, with LENTIS analogues showing differing consistent patterns.

The rainfall shows large variability between dynamically similar events (Figures S4–S12), as not every cut-off low-pressure system has associated rainfall and small shifts in the location of the cut-off low can lead to rainfall over a different area. Some individual analogues do show intense rainfall in the same region as the event (Figures S4–S12). The KNMI–LENTIS present period best captures the event itself; though we note the model is not at a convection-permitting resolution, suggesting the similarity comes from large-scale precipitation. Different trends are found in the reanalysis and model over the region most affected in July 2021 (Figure 5a–g)—the reanalysis shows a statistically significant rainfall increase, in agreement with Faranda et al. (2022). In contrast, the model shows a statistically significant decrease in rainfall over the impacted region, but an increase elsewhere. Both reanalysis and model show an increase in rainfall east of the region impacted in July 2021. In a region centred around the cut-off, low precipitation rates can be expected to increase. Thus, the shift in rainfall shown in the model is likely caused by the eastward shift in the centre of the low, shown in Figure 2.

To confirm that this shift occurs across all analogues the rainfall totals for each gridpoint within the two regions for all analogues is shown (Figure 5h–k). The eastern region shows an increase in intense rainfall, suggesting the region may need to prepare for more intense rainfall from summertime cut-off lows in the future. Analysis of different climate models could help improve certainty.

It is hard to assess precipitation changes through time due to the inhomogeneous and stochastic nature of rainfall. Total column water vapour provides a more homogeneous pattern, allowing assessment of whether analogues show the expected increase from Clausius–Clapeyron scaling or an accelerated change. We can only assess for ERA-5 (Figure 6), but find a 3.8% increase in total column water vapour over the analogue domain. The local temperature change between analogue sets over the domain is 0.5°C. Assuming an atmospheric water content increase of 7%/1°C warming, precipitable water increase between periods agrees with that expected from the warming atmosphere of ∼3–4% between the periods.

4 | DISCUSSION

We have used flow analogues to investigate climate change-induced changes in key characteristics of the atmospheric flow pattern associated with the July 2021 Western Europe flood event. We assess changes in intensity, frequency, and persistence in the dynamics of such events between past (1950–1979) and present (1993–2022) in reanalysis and present and future (+2K) in a climate model. From ERA-5 data, we find that the closest present-day analogues are more intense and more similar to the observed cut-off low-pressure of July 2021 than past analogues. Using 1600 simulated years from a 160-member ensemble (KNMI–LENTIS) for present-day and future climate, we show an intensification and eastward shift in the most similar low-pressure systems in the future—and an associated shift in rainfall. We show that similar events from both reanalysis and model datasets persist for far longer than the event did—suggesting longer-lasting cut-off lows are possible.

Next to those dynamic changes, we find an increase in total precipitable water in ERA-5 that follows expectations based on the Clausius–Clapeyron relationship. Assessing changes in precipitation consistent with the identified changes in streamfunction is more challenging. This is likely because localised precipitation is determined by more than large-scale circulation alone. The use of other methods, such as pseudo-global warming experiments (Lenderink et al., 2021; Schär et al., 1996), would enable further investigation of projected precipitation changes. However, with both the analogues method presented and pseudo global warming experiments, we are restricted to events that have been observed, but we are increasingly experiencing unprecedented climate extremes.

The method can be applied to many different climatic extremes—such as high-pressure systems, which frequently lead to extreme heat (White et al., 2023). Indeed, the analogue identification method is sensitive to sharp gradients thus, large-scale patterns associated with heatwaves may be more suited than most rainfall events (Holmberg et al., 2023). In addition, this method would be ideal to investigate atmospheric blocking events, which often cause impacts over Europe and future changes are not well understood (Kautz et al., 2022; Woollings et al., 2018). We find that the analogues do not all capture surface impacts, by extending the method to identify analogues based on multiple variables, for example, both streamfunction and precipitation, could

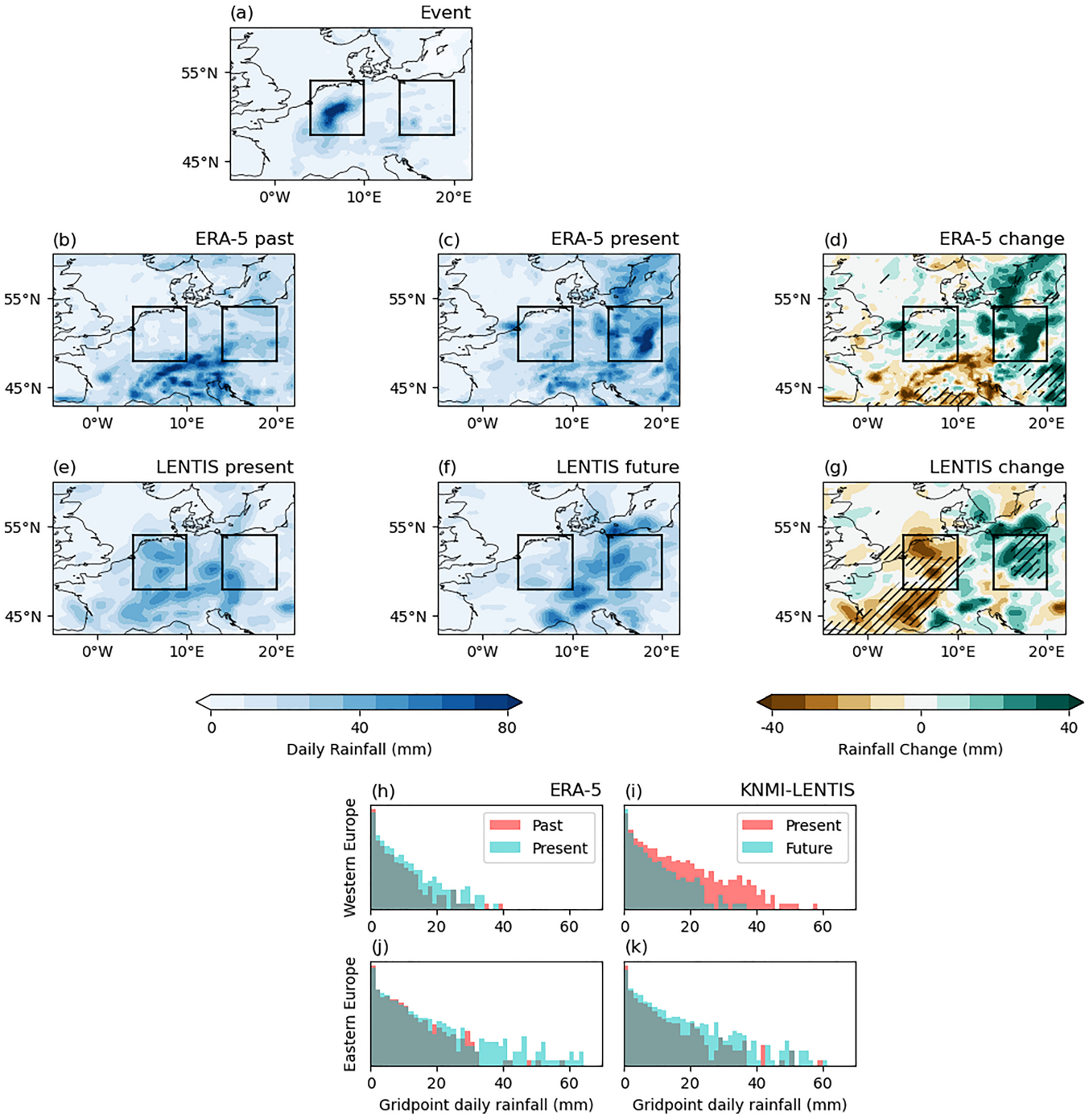

FIGURE 5 Rainfall of analogue events. (a) The daily rainfall totals of the observed event, 14 July 2021. (b, c) The gridpoint maximum of the daily rainfall from the analogue sets identified from 250 hPa streamfunction from ERA-5, past (1950–1979) and present (1993–2022). (d) The difference between the past and present, with hashed regions indicating statistically significant change between the time periods, calculated using a pointwise two-sided Welch's *t*-test with $p > 0.05$ deemed significant. (e–g) As in (b–d), but for the KNMI–LENTIS data, present (2000–2009) and future (2075–2084 in SSP2-4.5; 2K warmer). (h–k) Histograms of the frequency of gridpoint daily rainfall totals for the western (54° N–57° N, 4° E–10° E) and eastern (54° N–57° N, 14° E–20° E) Europe regions is shown in (a–g). Red is the past (present for LENTIS), and cyan is the present (future for LENTIS), a darker region where the two overlap.

enhance its value for impact studies. Investigating analogues identified based on one variable, but then also selecting based on another characteristic—such as persistence—would allow further investigation.

In this study, we have investigated only a single climate model large ensemble and only two periods of that model. Still, the fact that trends in reanalysis and in the model give similar patterns gives us confidence in our

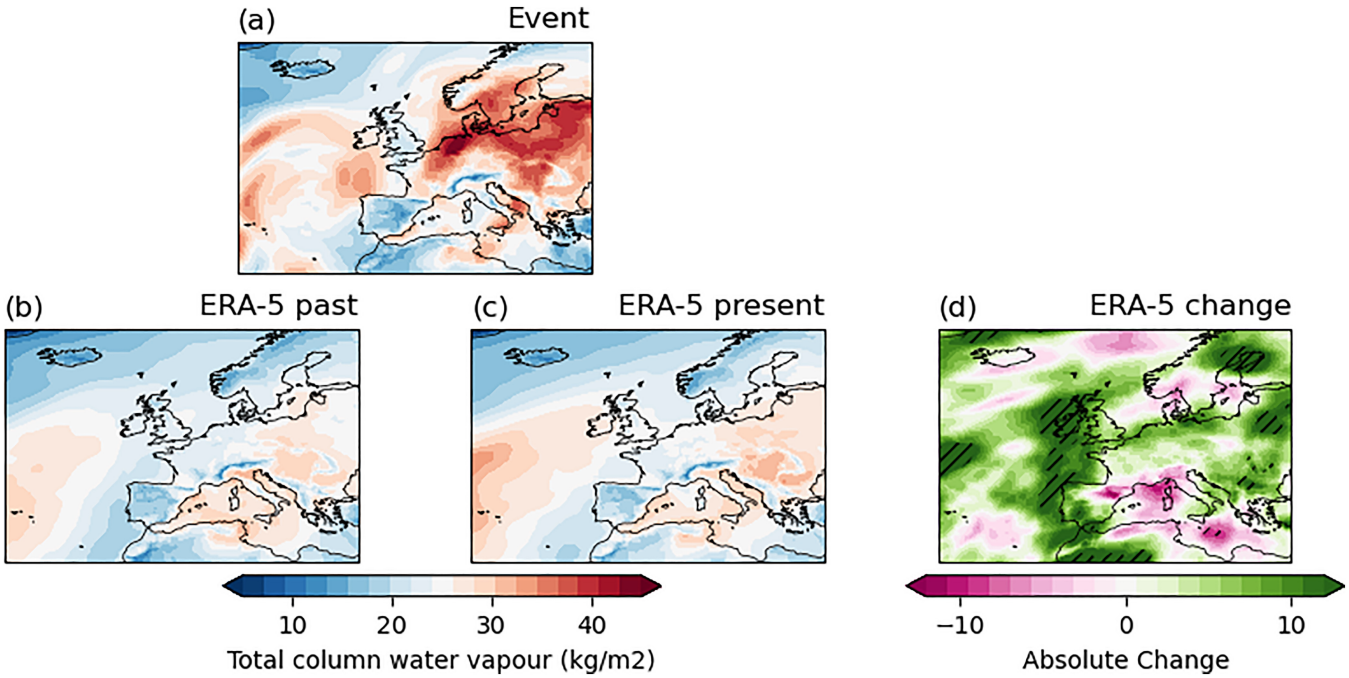

FIGURE 6 Total water column vapour of the reanalysis analogue events. (a) The total water column vapour of the observed event, 14 July 2021. (b, c) Composites of the total water column vapour from the analogue sets identified from 250 hPa streamfunction from ERA-5, past (1950–1979) and present (1993–2022). (d) The difference between the past and present, with hashed regions indicating statistically significant change between the time periods, calculated using a pointwise two-sided Welch's *t*-test with $p > 0.05$ deemed significant.

findings. To increase the generalisability of the conclusions, multiple climate models should be assessed, for example, using the large ensemble single forcing model intercomparison project (Smith et al., 2022).

Assessing flow analogues is not useful for every extreme, as some events are too unusual. As the climate changes, there may be some events with suitable analogues in the present—but not in the past. In those cases, analogues can be used to show the event likelihood is increasing, but not to examine changes in intensity or persistence. Our results show that future European summertime cut-off lows could be more extreme than experienced so far and could occur more often—potentially causing greater impacts. Through adaptation we can reduce impacts of possible future events on both society and environment.

AUTHOR CONTRIBUTIONS

Vikki Thompson: Methodology; formal analysis; writing – original draft; writing – review and editing. **Dim Coumou:** Conceptualization; supervision; formal analysis; writing – review and editing. **Vera Melinda Galfi:** Writing – review and editing; formal analysis. **Tamara Happé:** Formal analysis; writing – review and editing. **Sarah Kew:** Formal analysis; conceptualization; writing – review and editing. **Izidine Pinto:** Formal analysis; writing – review and editing. **Sjoukje Philip:** Conceptualization; formal analysis; writing – review and editing. **Hylke de Vries:** Conceptualization; formal analysis; writing – review and editing. **Karin van der Wiel:** Conceptualization; formal analysis; writing – review and editing.

ACKNOWLEDGEMENTS

We are grateful to our two anonymous reviewers, whose careful comments improved the manuscript. This research has been supported by the KNMI multi-year strategic research funding (grant name MSO-Extreme-Weather). This study was partly supported by the European Union's Horizon 2020 research and innovation programme under grant agreement No 101003469 (XAIDA project).

DATA AVAILABILITY STATEMENT

ERA5 data are available from the European Centre for Medium-Range Weather Forecasts (ECMWF), Copernicus Climate Change Service (C3S) at Climate Data Store (CDS; https://cds.climate.copernicus.eu/). The KNMI–LENTIS dataset description is recorded on Zenodo (https://doi.org/10.5281/zenodo.7573137, Muntjewerf et al., 2023b), providing details of the layout of the dataset, where it is located, how it is stored, and how one gains access. The code used to generate the figures in this paper and the Supporting Information Materials is

available from github and zenodo: [https://github.com/vikki-thompson/analogues_2024 and https://doi.org/10.5281/zenodo.13143914]. All data needed to evaluate the conclusions in the paper are present in the paper and/or the Supporting Information Materials.

ORCID

Vikki Thompson https://orcid.org/0000-0002-1650-7354
Tamara Happé https://orcid.org/0000-0002-4548-506X
Sarah Kew https://orcid.org/0000-0003-3210-7040
Izidine Pinto https://orcid.org/0000-0002-9919-4559

REFERENCES

Bell, B., Hersbach, H., Simmons, A., Berrisford, P., Dahlgren, P., Horányi, A. et al. (2021) The ERA5 global reanalysis: preliminary extension to 1950. *Quarterly Journal of the Royal Meteorological Society*, 147(741), 4186–4227. Available from: https://doi.org/10.1002/qj.4174

Di Capua, G. & Rahmstorf, S. (2023) Extreme weather in a changing climate. *Environmental Research Letters*, 18(10), 102001. Available from: https://doi.org/10.1088/1748-9326/acfb23

Döscher, R., Acosta, M., Alessandri, A., Anthoni, P., Arsouze, T., Bergman, T. et al. (2022) The EC-Earth3 Earth system model for the Coupled Model Intercomparison Project 6. *Geoscientific Model Development*, 15, 2973–3020. Available from: https://doi.org/10.5194/gmd-15-2973-2022

Faranda, D., Bourdin, S., Ginesta, M., Krouma, M., Noyelle, R., Pons, F. et al. (2022) A climate-change attribution retrospective of some impactful weather extremes of 2021. *Weather and Climate Dynamics*, 3(4), 1311–1340. Available from: https://doi.org/10.5194/wcd-3-1311-2022

Fischer, E. & Knutti, R. (2016) Observed heavy precipitation increase confirms theory and early models. *Nature Climate Change*, 6, 986–991. Available from: https://doi.org/10.1038/nclimate3110

Fowler, H.J., Lenderink, G., Prein, A.F., Westra, S., Allan, R.P., Ban, N. et al. (2021) Anthropogenic intensification of short-duration rainfall extremes. *Nature Reviews Earth & Environment*, 2(2), 107–122. Available from: https://doi.org/10.1038/s43017-020-00128-6

Holmberg, E., Messori, G., Caballero, R. & Faranda, D. (2023) The link between European warm-temperature extremes and atmospheric persistence. *Earth System Dynamics*, 14(4), 737–765. Available from: https://doi.org/10.5194/esd-14-737-2023

Jézéquel, A., Yiou, P. & Radanovics, S. (2018) Role of circulation in European heatwaves using flow analogues. *Climate Dynamics*, 50, 1145–1159. Available from: https://doi.org/10.1007/s00382-017-3667-0

Kahraman, A., Kendon, E.J., Chan, S.C. & Fowler, H.J. (2021) Quasi-stationary intense rainstorms spread across Europe under climate change. *Geophysical Research Letters*, 48, e2020GL092361. Available from: https://doi.org/10.1029/2020GL092361

Kautz, L.A., Martius, O., Pfahl, S., Pinto, J.G., Ramos, A.M., Sousa, P.M. et al. (2022) Atmospheric blocking and weather extremes over the Euro-Atlantic sector—a review. *Weather and Climate Dynamics*, 3(1), 305–336. Available from: https://doi.org/10.5194/wcd-3-305-2022

Koks, E.E., van Ginkel, K.C.H., van Marle, M.J.E. & Lemnitzer, A. (2022) Brief communication: critical infrastructure impacts of the 2021 mid-July Western European flood event. *Natural Hazards and Earth System Sciences*, 22, 3831–3838. Available from: https://doi.org/10.5194/nhess-22-3831-2022

Lenderink, G., de Vries, H., Fowler, H.J., Barbero, R., van Ulft, B. & van Meijgaard, E. (2021) Scaling and responses of extreme hourly precipitation in three climate experiments with a convection-permitting model. *Philosophical Transactions A*, 379(2195), 20190544.

Masson-Delmotte, V., Zhai, P., Pirani, A., Connors, S.L., Péan, C., Berger, S. et al. (2021) Climate change 2021: the physical science basis. In: *Contribution of working group I to the sixth assessment report of the Intergovernmental Panel on Climate Change*. Cambridge: Cambridge University Press.

Mohr, S., Ehret, U., Kunz, M., Ludwig, P., Caldas-Alvarez, A., Daniell, J.E. et al. (2023) A multi-disciplinary analysis of the exceptional flood event of July 2021 in central Europe. Part 1: event description and analysis. *Natural Hazards and Earth System Sciences Discussions*, 23, 525–551. Available from: https://doi.org/10.5194/nhess-23-525-2023

Muntjewerf, L., Bintanja, R., Reerink, T. & van der Wiel, K. (2023a) The KNMI large ensemble time slice (KNMI–LENTIS). *Geoscientific Model Development*, 16, 4581–4597. Available from: https://doi.org/10.5194/gmd-16-4581-2023

Muntjewerf, L., Bintanja, R., Reerink, T. & van der Wiel, K. (2023b) KNMI-LENTIS large ensemble time slice dataset description. Zenodo. https://doi.org/10.5281/zenodo.7573137

Noyelle, R., Zhang, Y., Yiou, P. & Faranda, D. (2023) Maximal reachable temperatures for Western Europe in current climate. *Environmental Research Letters*, 18, 094061. Available from: https://doi.org/10.1088/1748-9326/acf679

Otto, F.E., van der Wiel, K., van Oldenborgh, G.J., Philip, S., Kew, S.F., Uhe, P. et al. (2018) Climate change increases the probability of heavy rains in Northern England/Southern Scotland like those of storm Desmond—a real-time event attribution revisited. *Environmental Research Letters*, 13(2), 024006. Available from: https://doi.org/10.1088/1748-9326/aa9663

Philip, S., Kew, S.F., van Oldenborgh, G.J., Aalbers, E., Vautard, R., Otto, F. et al. (2018) Validation of a rapid attribution of the May/June 2016 flood-inducing precipitation in France to climate change. *Journal of Hydrometeorology*, 19(11), 1881–1898. Available from: https://doi.org/10.1175/JHM-D-18-0074.1

Rajczak, J. & Schär, C. (2017) Projections of future precipitation extremes over Europe: a multimodel assessment of climate simulations. *Journal of Geophysical Research: Atmospheres*, 122(20), 10773–10800. Available from: https://doi.org/10.1002/2017JD027176

Schär, C., Frei, C., Lüthi, D. & Davies, H.C. (1996) Surrogate climate-change scenarios for regional climate models. *Geophysical Research Letters*, 23, 669–672.

Schulzweida, U. (2023) CDO user guide. https://doi.org/10.5281/ZENODO.10020800

Seneviratne, S.I., Zhang, X., Adnan, M., Badi, W., Dereczynski, C., Di Luca, A. et al. (2021) Weather and climate extreme events in a changing climate. Climate change 2021: the physical science basis. In: Masson-Delmotte, V., Zhai, P., Pirani, A., Connors, S.-L., Péan, C., Berger, S. et al. (Eds.) *Contribution of working group I to the sixth assessment report of the Intergovernmental Panel on Climate Change*. Cambridge: Cambridge University Press. Available from: https://www.ipcc.ch/

Smith, D.M., Gillett, N.P., Simpson, I.R., Athanasiadis, P.J., Baehr, J., Bethke, I. et al. (2022) Attribution of multi-annual to decadal changes in the climate system: the large ensemble single forcing model intercomparison project (LESFMIP). *Frontiers in Climate*, 4, 955414.

Tradowsky, J.S., Philip, S.Y., Kreienkamp, F., Kew, S.F., Lorenz, P., Arrighi, J. et al. (2023) Attribution of the heavy rainfall events leading to severe flooding in Western Europe during July 2021. *Climatic Change*, 176, 90. Available from: https://doi.org/10.1007/s10584-023-03502-7

van de Vyver, H., van Schaeybroeck, B., de Cruz, L., Hamdi, R. & Termonia, P. (2023) Bias-adjustment methods for future subdaily precipitation extremes consistent across durations. *Earth and Space Science*, 10(3), e2022EA002798. Available from: https://doi.org/10.1029/2022EA002798

van der Wiel, K., Beersma, J., van den Brink, H., Krikken, F., Selten, F., Severijns, C. et al. (2024) KNMI'23 climate scenarios for the Netherlands: storyline scenarios of regional climate change. *Earth's Future*, 12(2), e2023EF003983.

van der Wiel, K., Kapnick, S.B., van Oldenborgh, G.J., Whan, K., Philip, S., Vecchi, G.A. et al. (2017) Rapid attribution of the August 2016 flood-inducing extreme precipitation in south Louisiana to climate change. *Hydrology and Earth System Sciences*, 21(2), 897–921. Available from: https://doi.org/10.5194/hess-21-897-2017

van Oldenborgh, G.J., van der Wiel, K., Sebastian, A., Singh, R., Arrighi, J., Otto, F. et al. (2017) Attribution of extreme rainfall from hurricane Harvey, August 2017. *Environmental Research Letters*, 12(12), 124009.

van Oldenborgh, G.J., Wehner, M.F., Vautard, R., Otto, F.E., Seneviratne, S.I., Stott, P.A. et al. (2022) Attributing and projecting heatwaves is hard: we can do better. *Earth's Future*, 10(6), e2021EF002271. Available from: https://doi.org/10.1029/2021EF002271

White, R.H., Anderson, S., Booth, J.F., Braich, G., Draeger, C., Fei, C. et al. (2023) The unprecedented Pacific Northwest heatwave of June 2021. *Nature Communications*, 14(1), 727. Available from: https://doi.org/10.1038/s41467-023-36289-3

Woollings, T., Barriopedro, D., Methven, J., Son, S.W., Martius, O., Harvey, B. et al. (2018) Blocking and its response to climate change. *Current Climate Change Reports*, 4, 287–300. Available from: https://doi.org/10.1007/s40641-018-0108-z

Yiou, P., Salameh, T., Drobinski, P., Menut, L., Vautard, R. & Vrac, M. (2013) Ensemble reconstruction of the atmospheric column from surface pressure using analogues. *Climate Dynamics*, 41, 1333–1344. Available from: https://doi.org/10.1007/s00382-012-1626-3

SUPPORTING INFORMATION

Additional supporting information can be found online in the Supporting Information section at the end of this article.

How to cite this article: Thompson, V., Coumou, D., Galfi, V. M., Happé, T., Kew, S., Pinto, I., Philip, S., de Vries, H., & van der Wiel, K. (2024). Changing dynamics of Western European summertime cut-off lows: A case study of the July 2021 flood event. *Atmospheric Science Letters*, *25*(10), e1260. https://doi.org/10.1002/asl.1260